J Mater Sci (2010) 45:1227–1230
DOI 10.1007/s10853-009-4069-4

A comparison of results obtained using different methods to assess the elastic properties of ceramic materials exemplified for $Ba_{0.5}Sr_{0.5}Co_{0.8}Fe_{0.2}O_{3-\delta}$

J. Malzbender · B. Huang · J. Mönch · R. W. Steinbrech

Received: 31 July 2009 / Accepted: 22 November 2009 / Published online: 4 December 2009

Abstract Different mechanical testing methods have been used to assess the elastic behavior of the mixed ion electron conducting perovskite $Ba_{0.5}Sr_{0.5}Co_{0.8}Fe_{0.2}O_{3-\delta}$ (BSCF). Although the main aim is the comparison of the testing techniques for ceramic material in general, experiments have been performed at RT and up to 900 °C to illustrate the capabilities of the utilized methods for a perovskite with a stiffness anomaly. BSCF specimens in disc shape and tubular geometry provided by different suppliers were tested in biaxial bending by ring-on-ring testing and under uniaxial stress in O-ring and under compression loading. The elastic modulus was determined as a function of temperature up to 900 °C. In addition, the room temperature elastic modulus was measured using depth-sensitive indentation.

Introduction

The elastic modulus is an important parameter in the analysis and modeling of the mechanical behavior of materials which is related to the deformation, stress development, and failure [1]. Various integral mechanical methods have been developed, which are based on the elastic response of entire specimens upon loading. Since tensile testing of ceramics has difficulties associated with the brittle behavior of the materials, the elastic deformation of ceramic materials is typically analyzed in bending or compression tests [2, 3]. These global tests result in a good representation of the macroscopic behavior whereas the local deformation on a microstructure-scale is typically tested using microindentation [4, 5]. However, investigations which comprise for the same material a comparison of both macro- and microtesting results are limited [6]. In this paper such a comparison is carried out for a perovskite ceramic considered as a candidate material for gas separation.

The interest in perovskites of ABO_3 type (rare earth metal ions in A sites, and transition metal ions in B sites) for potential applications in gas separation membranes has increased in recent years [7]. Oxyfuel technology is an important option for the carbon capture and storage (CCS) strategy in order to reduce CO_2 emissions from point sources such as fossil fuelled power plants. The required oxygen can be provided by ceramic membranes, which are assumed to have lower losses compared to cryogenic air liquefaction. When operated at high temperature, the mixed ionic and electronic conducting perovskite membranes can selectively separate oxygen from air by the diffusion of oxygen ions. The mechanism is based on the interaction of gaseous oxygen with the oxide lattice [8]. The difference of chemical potential of oxygen provides the driving force. Among ABO_3 perovskites the $Ba_{0.5}Sr_{0.5}Co_{0.8}Fe_{0.2}O_{3-\delta}$ compound exhibits excellent electronic and ionic conductivity [9, 10].

Characterization of the elastic behavior of ceramic gas separation membranes is one of the tasks in the MEM-BRAIN Project of the Helmholtz—Association [11]. Thus, the comparison of the stiffness testing methods was exemplified in the context of this project. This work compares the elastic modulus of $Ba_{0.5}Sr_{0.5}Co_{0.8}Fe_{0.2}O_{3-\delta}$ determined using biaxial bending in ring-on-ring loading,

J. Malzbender (✉) · B. Huang · J. Mönch · R. W. Steinbrech
Forschungszentrum Jülich GmbH, IEF-2, 52425 Jülich, Germany
e-mail: j.malzbender@fz-juelich.de

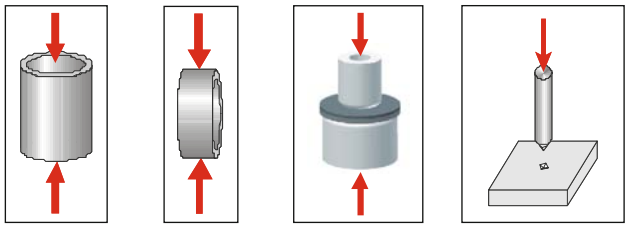

Fig. 1 Characterization methods **a** compression test, **b** O-ring test, **c** ring-on-ring test, and **d** indentation

the complex stress field of an O-ring tests, compression tests, and depth-sensitive microindentation (Fig. 1). In the macroscopic tests, the elastic modulus was determined as a function of temperature in air up to 900 °C.

Hence, the aim of this work is in addition to a comparison of testing methods in general also to test the effect of the specimen geometry (flat plate, tubular), the specimen volume (small—indentation, larger—compression, ring-on-ring, O-ring), the stress state (uniaxial—compression, biaxial and combined tension and compression—ring-on-ring, O-ring, biaxial large stresses—indentation). Furthermore, the effect of temperature variations on the testing method is assessed. The current work also summarizes relevant relationships for ring-on-ring and O-ring testing (with a reference to C-ring testing).

Experiments

Tubular and disc-shaped $Ba_{0.5}Sr_{0.5}Co_{0.8}Fe_{0.2}O_{3-\delta}$ samples were provided by different suppliers. The tubular specimens were prepared by an extrusion process by HITK (Hermsdorfer Institut für Technische Keramik, Hermsdorf, Germany). The tubes were cut into smaller segments and O-rings. In addition, disc-shaped samples were available from HITK and IEF-1 (Forschungszentrum Jülich). The discs were uniaxially pressed by powder compaction without any additive.

Depth-sensitive microindentation was used to determine the local stiffness. The stiffness was derived from the unloading slope of the indentation load–displacement curves measured using a Fischerscope with Vickers diamond tip indenter. The elastic modulus was determined following the Oliver and Pharr procedure [4].

The disc-shaped samples were loaded in biaxial ring-on-ring bending tests. The stiffness of the specimens was measured at different temperatures. The testing conditions followed the procedures recommended in the ASTM standard C 1499-05 [2]. The stiffness was calculated using the equations for linear bending theory [3]:

$$E = \frac{3(1-\nu^2)\cdot r_1^2\cdot \Delta P}{2\pi\cdot \Delta d\cdot t^3}\left[\left(\frac{r_2}{r_1}\right)^2 - 1 - \ln\left(\frac{r_2}{r_1}\right) + \frac{1}{2}\left(\frac{1-\nu}{1+\nu}\right)\cdot\left(\frac{(r_2^2-r_1^2)^2}{r_2^2 r_3^2}\right)\right], \quad (1)$$

where P is the applied force, t the specimen thickness, ν the Poisson ratio, and r_1, r_2, and r_3 the radii of the load ring, supporting ring, and (circular) specimen, respectively, d the central deflection of the specimen. In this work, t, r_1, r_2, and r_3 take a value of 1.05, 9, 18.6, and 21.78 mm for the IEF-1 specimens and 1.03, 1.65, 5, and 7.85 mm for the HITK specimens. The loading rate was 100 N/min in all tests.

Relationships to determine the stiffness from the load–displacement curves obtained for tubular specimens in O- and C-ring geometry are given in [12]. Hence, in the O-ring test the elastic modulus was determined after [12]:

$$E = \frac{\Delta P\cdot r^2}{\Delta d\cdot b\cdot t\cdot e}\left\{\frac{\pi}{4} - \frac{2}{\pi}\left(1-\frac{e^2}{r^2}\right) + 2\frac{e}{r}\left[\frac{2}{\pi}\left(1-\frac{e}{r}\right) - \frac{\pi}{8}\right] + 1.9\cdot(1+\nu)\cdot\frac{e}{r}\right\}, \quad (2)$$

where r is the radius of the tubular specimen (inner radius 6.5 mm, outer radius 7.5 mm), the neutral axis e is defined as $e = r - h(\ln(r+h/2)/r-h/2))^{-1}$. The width of the specimens was 4 mm in these tests.

In the compressive test, tubular specimens with the length of 30 mm were used. The stiffness of the material was characterized at different temperatures in the range RT to 900 °C. For the tests at elevated temperatures, a heating/cooling rate of 8 K/min was used. The samples were heated to 900 °C followed by a dwell time of 40 min to reach thermal equilibrium before testing. The displacement was measured using a mechanical sensor.

Results and discussion

The stiffness was measured by indenting polished cross sections that were mounted in epoxy. The flat IEF-1 specimens that were prepared using hot pressing did not reveal any stiffness anisotropy with an average elastic modulus of ~78 GPa in the load range 50–400 mN that decreased slightly by ~10% up to 1000 mN (Fig. 2).

The extruded HITK tubes exhibited different elastic properties close to both surfaces as measured with indentation (Fig. 2). The stiffness values near the outer surface were 20% higher; ~90 GPa compared to ~67 GPa near the inner surface (100 mN). At higher indentation loads (1000 mN), the values decreased to ~70 GPa and ~60 GPa for the outer and inner surface, respectively. The

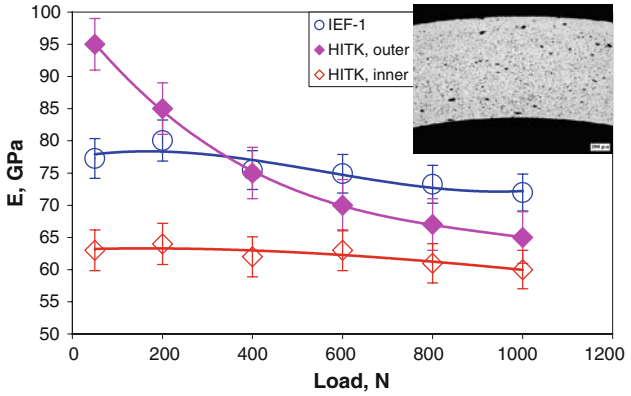

Fig. 2 Elastic modulus as a function of load for material from IEF-1 and HITK as obtained using indentation testing. An optical micrograph of a cross section of a HITK tube is provided as an insert. An approximately 100 μm layer with lower porosity can be seen near the outer surface of the tube

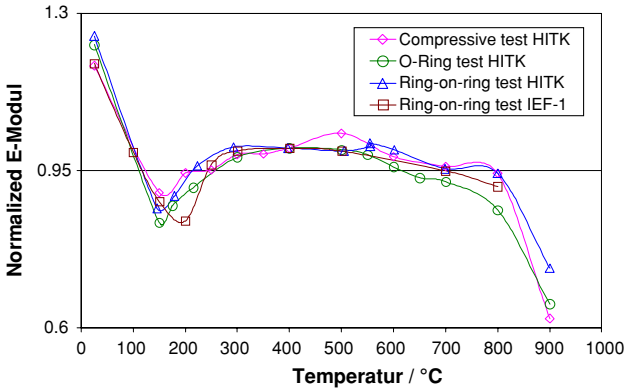

Fig. 3 Stiffness normalized with respect to the value obtained at 400 °C as a function of temperature obtained using the different characterization methods

higher value near the outer surface of the tube is a result of a thin layer of lower porosity near the outer surface of the tubes (Fig. 2) resulting from the extrusion process.

The results reveal that inhomogeneities from the preparation process can be traced, but caution is advised with respect to possible indentation size effects, since at low loads the individual grains are tested and the effect of grain-boundaries and defects (e.g., pores) will be underestimated the stiffness measured at 1000 mN appears to be more representative for the materials behavior.

In Table 1, the indentation stiffness results are compared with those of the global measurements for the BSCF of both suppliers. The room temperature stiffness values are in the range of 60–70 GPa. There is fairly good agreement between the results of the different testing methods and the two BSCF variants. RT values of 60–90 GPa have been reported for BSCF in literature [13].

The normalized stiffness as a function of temperature obtained using the different integral (global) characterization methods is presented in Fig. 3, where it can be seen that there is good agreement in the temperature dependency of the stiffness as assessed using the different methods. The ratio of the value at 900 °C to the RT stiffness is ~0.45.

Table 1 Comparison of stiffness results determined with the different mechanical methods (average experimental uncertainty 7%)

Method	Geometry	Stiffness, GPa	
		HITK	IEF-2
Compressive test	Tube	68	–
Ring-on-ring	Disc	68	63
O-ring	Ring from tube	62	–
Indentation	Disc	61[a]	70

[a] 1000 mN, not representative for the outer side of the tube

A value of ~0.35 has been reported for BSCF [14]. The temperature dependency is invariant to the different stress states (uniaxial as compared to biaxial). An initial decrease of the stiffness is observed with a minimum at ~200 °C and a second decrease around 700–800 °C (Fig. 3). Note that although the load–deflection curves obtained in these tests were linear and did not reveal any indication of nonelastic deformation, a decrease in measured stiffness due to creep deformation at 900 °C cannot be ruled out. The reasons for these stiffness changes that might be related with changes in phases composition, structure or stoichiometry are still under investigation and will be published separately [15]. The O-ring testing of the BSCF variants from HITK leads to lower values (Table 1).

Conclusions

Different methods were used to assess the stiffness of BSCF specimens. The preparation method, i.e., extrusion as compared to hot pressing did not influence the materials properties. Although the stress field in terms of the combination of compressive and tensile stresses as compared to pure compressive stress differs in these testing methods, there was overall agreement with respect to the determined stiffness as well as its temperature dependence. This implies that the material does not experience a stress dependent stiffness changes under the testing conditions. Furthermore, it is important to note that indentation testing reveals additional information with respect to local stiffness variations regarding the sample surface.

Acknowledgements The work was funded by the German Helmholtz Gemeinschaft as part of the research activities in the MEMBRAIN Alliance. The authors would like to express their gratitude to R. Kriegel, I. Voigt (HITK) and W. Meulenberg, S. Baumann (FZ Jülich, IEF-1) for providing the BSCF specimens and B. Rutkowski for the optical micrograph of the HITK tube.

References

1. de With G (2006) Structure, deformation, and integrity of materials. Wiley-VSH, Weinheim
2. ASTM Standard C1499-05 (2005) ASTM International, West Conshohoken, PA
3. Schmitt RW, Schönbrunn G (1983) Sprechsaal 116:387
4. Oliver WC, Pharr GM (1992) J Mater Res 7:1564
5. Malzbender J, den Toonder JMJ, Balkenende AR, de With G (2002) Mater Sci Eng Rep 36:47
6. Malzbender J, Steinbrech RW (2003) J Mater Res 18:1975
7. Cheng JH, Navrotsky A (2005) Chem Mater 17:2197
8. Bouwmeester HJM, Burgraaf AJ (1997) In: Gellings PJ, Bouwmeester HJM (eds) CRC handbook of solid state electrochemistry. CRC Press Inc, New York
9. Shao Z, Xiong G, Tong J, Dong H, Yang W (2001) Separ Purif Technol 25:419
10. Vente JF, McIntosh S, Haije WG, Bouwmeester HJM (2006) J Solid State Electrochem 10:581
11. Czyperek M, Zapp P, Bouwmeester HJM, Modigell M, Peinemann K-V, Voigt I, Meulenberg WA, Singheiser L, Stöver D (2009) Energy Procedia 1:303
12. Bongartz K, Gyarmati E, Schuster H, Tauber K (1976) J Nucl Mater 62:123
13. Pfaff EM, Zwick M (2008) In: Lara-Curzio E (ed) Mechanical properties and performance of engineering ceramics and composites III, Wiley, USA, 21 p
14. Pfaff EM, Zwick M (2008) Membrane Summer School. http://www.fz-juelich.de/ief/ief-1/datapool/page/284//Summer_School_2008_Pfaff.pdf
15. Huang BX, Malzbender J, Steinbrech RW, Grychtol P, Schneider CM, Singheiser L (2009) Appl Phys Lett 95:051901